Conduction through the inward rectifier potassium channel, Kir2.1, is increased by negatively charged extracellular residues

Nazzareno D'Avanzo
Hee Cheol Cho, *Emory University*
Illya Tolokh
Roman Pekhletski
Igor Tolokh
Chris Gray
Saul Goldman
Peter H. Backx

Journal Title: Journal of General Physiology
Volume: Volume 125, Number 5
Publisher: Rockefeller University Press | 2005-05-01, Pages 493-503
Type of Work: Article | Final Publisher PDF
Publisher DOI: 10.1085/jgp.200409175
Permanent URL: https://pid.emory.edu/ark:/25593/s7803

Final published version: http://dx.doi.org/10.1085/jgp.200409175

Conduction through the Inward Rectifier Potassium Channel, Kir2.1, Is Increased by Negatively Charged Extracellular Residues

Nazzareno D'Avanzo,[1] Hee Cheol Cho,[2] Illya Tolokh,[3] Roman Pekhletski,[1] Igor Tolokh,[3] Chris Gray,[3] Saul Goldman,[3] and Peter H. Backx[1]

[1]Department of Physiology and Medicine and Department of Heart and Stroke, Richard Lewar Centre, University of Toronto, Toronto, Ontario M5S 3E2, Canada

[2]Institute of Molecular Cardiobiology, Johns Hopkins University, Baltimore, MD 21218

[3]Department of Chemistry and Department of Physics, University of Guelph, Guelph, Ontario N1G 2W1, Canada

ABSTRACT Ion channel conductance can be influenced by electrostatic effects originating from fixed "surface" charges that are remote from the selectivity filter. To explore whether surface charges contribute to the conductance properties of Kir2.1 channels, unitary conductance was measured in cell-attached recordings of Chinese hamster ovary (CHO) cells transfected with Kir2.1 channels over a range of K^+ activities (4.6–293.5 mM) using single-channel measurements as well as nonstationary fluctuation analysis for low K^+ activities. K^+ ion concentrations were shown to equilibrate across the cell membrane in our studies using the voltage-sensitive dye $DiBAC_4(5)$. The dependence of γ on the K^+ activity (a_K) was fit well by a modified Langmuir binding isotherm, with a nonzero intercept as a_K approaches 0 mM, suggesting electrostatic surface charge effects. Following the addition of 100 mM *N*-methyl-D-glucamine (NMG^+), a nonpermeant, nonblocking cation or following pretreatment with 50 mM trimethyloxonium (TMO), a carboxylic acid esterifying agent, the γ–a_K relationship did not show nonzero intercepts, suggesting the presence of surface charges formed by glutamate or aspartate residues. Consistent with surface charges in Kir2.1 channels, the rates of current decay induced by Ba^{2+} block were slowed with the addition of NMG or TMO. Using a molecular model of Kir2.1 channels, three candidate negatively charged residues were identified near the extracellular mouth of the pore and mutated to cysteine (E125C, D152C, and E153C). E153C channels, but not E125C or D152C channels, showed hyperbolic γ–a_K relationships going through the origin. Moreover, the addition of MTSES to restore the negative charges in E53C channels reestablished wild-type conductance properties. Our results demonstrate that E153 contributes to the conductance properties of Kir2.1 channels by acting as a surface charge.

KEY WORDS: surface charges • Kir2.1 • conduction • NMG • TMO

INTRODUCTION

Electrostatic forces originating from charged groups on protein surfaces influence a variety of macromolecular functions. For example, charges on the surface of superoxide dismutases provides electrostatic guidance for substrates entering the active site (Getzoff et al., 1983, 1992; Sharp et al., 1987). Surface charges have also been shown to affect channel conductance in a variety of ion channels, such as neuronal Na^+ channels (Sigworth and Spalding, 1980; Worley et al., 1986), Ca^{2+}-activated K^+ (BK) channels (MacKinnon and Miller, 1989; MacKinnon et al., 1989), and nicotinic acetylcholine receptors (NAChR) (Imoto et al., 1988; Konno et al., 1991), presumably by influencing the permeant ion concentration of ions at the entrance of the selectivity filter (Apell et al., 1977). In BK channels, surface charges also act to increase the affinity of cationic pore blockers by altering the local electrostatic potential at the pore entrance (MacKinnon and Miller, 1989; MacKinnon et al., 1989), while the "ring" of negative surface charges in NAChRs modifies the affinity of the pore blocker, Mg^{2+} (Imoto et al., 1988; Konno et al., 1991).

I_{K1} currents are found in many tissues and are generated by Kir2.x channels. In heart, a major molecular component of I_{K1} is the Kir2.1 channel (Zobel et al., 2003) and mutations in Kir2.1 channels have been linked to a form of long QT syndrome (LQT7) known as Andersen's syndrome (Plaster et al., 2001). Levels of I_{K1} in cardiomyocytes provide background K^+ currents that are involved in setting the resting membrane potential, preventing membrane hyperpolarization due to Na^+ pump activity, influencing propagation velocity, altering the electrical space constant, and promoting late phase

N. D'Avanzo and H.C. Cho contributed equally to this project.

Correspondence to Peter H. Backx: p.backx@utoronto.ca

Abbreviations used in this paper: CHO, Chinese hamster ovarian; $DiBAC_4(5)$, *bis*-(1,3-dibutylbarbituric acid)pentamethine oxonol; GCS, Gouy-Chapman-Stern; NAChR, nicotinic acetylcholine receptor; NMG, *N*-methyl-D-glucamine; NSFA, nonstationary fluctuation analysis; TMO, trimethyloxonium; WT, wild-type.

J. Gen. Physiol. © The Rockefeller University Press • 0022-1295/2005/05/493/11 $8.00
Volume 125 May 2005 493–503
http://www.jgp.org/cgi/doi/10.1085/jgp.200409175

repolarization. Consistent with an important role for I_{K1} in the heart, reductions in I_{K1} have been implicated in heart failure, and triggered arrhythmias resulting from early or delayed after-depolarizations observed in heart disease (Beuckelmann et al., 1993; Kääb et al., 1996; Puglisi et al., 2000; Pogwizd et al., 2001). On the other hand, blockade of I_{K1} is a potent inhibitor of reentry type arrhythmias and ventricular fibrillation by increasing electrical space constants (Qi et al., 2002). I_{K1} channels also play a critical role in conditions of ischemia and hypoxia, where $[K^+]_o$ is often elevated from 4 mM to as high as 20 mM (Weiss and Lamp, 1989), resulting in membrane potential depolarization as a consequence of the anomalous crossover properties of I_{K1} channels (Matsuda, 1991; Lopatin and Nichols, 1996).

The recent crystallography of the bacterial inward rectifier channel *KcsA* (Doyle et al., 1998) has provided important new insights into the molecular and biophysical mechanisms underlying the function of K^+ channels. Indeed, crystallography and molecular dynamic models have revealed important channel properties such as ion occupancy and unitary conductance as well mechanisms for ion permeation (Berneche and Roux, 2001, 2003; Morais-Cabral et al., 2001). While previous reports of the γ versus K^+ activity relationship in Kir2.1 channels were dedicated to studying the validity of various permeation models (Stampe et al., 1998), no studies have specifically examined the role of surface charges in Kir2.1 channel function.

In this study, we examined the conduction properties of the Kir2.1 channel over a range of K^+ activities using single-channel recordings and nonstationary fluctuation analysis. We employed three experimental strategies to alter surface charges in Kir2.1 channels: variation of the bulk solution ionic strength, surface charge neutralization, and site-directed mutagenesis. Our results establish a critical role for surface charges near the extracellular entrance of the pore in Kir2.1 channels originating from E153 residues to the conduction properties of K^+ ions. It will be necessary to consider the effect of E153 residues on ion occupancy and permeation in future studies.

MATERIALS AND METHODS

Expression of Mouse Kir2.1 Channels in Chinese Hamster Ovary (CHO) K1 Cells

Mouse Kir2.1 cDNA (a gift from L. Jan, Howard Hughes Medical Institute, San Francisco, CA) was subcloned into a bidirectional paBi-G vector (CLONTECH Laboratories, Inc.) modified by us to contain GFP (paBi-EGFP) (Zobel et al., 2003) in a TetOFF system requiring activation of the promoter by tetracycline transactivator (tTA) (CLONTECH Laboratories, Inc.). CHO-K1 cells were incubated at 37°C, 5% CO_2 in F12 media (Sigma-Aldrich), supplemented with 5% FBS and 1% penicillin/streptomycin (GIBCO BRL) and transfected with 2 μg of Kir2.1 cDNA plus 1 μg of tTA cDNA using 4 μl of Lipofectamine 2000 (GIBCO BRL) following the supplied protocol. Transfected cells were incubated in supplemented culture media (see below) for 24 h before the electrophysiological recordings. Single mutants were created on a four cysteine knockout background (4CKO = C89S/C101S/C149Y/C169S) via the Kunkel method.

Cell-attached Macropatch Recordings for Unitary Conductance

Electrophysiological recordings were done using the cell-attached patch clamp technique. Bath solutions contained (in mM) 2 $MgCl_2$, 10 HEPES, and 5–400 K^+ (Cl^- and OH^-) (pH 7.4, with KOH). The osmolarity was maintained when necessary by the addition of varying amounts of glucose. Pipette solutions had the same composition as the bath solutions, except $MgCl_2$ was removed and 1–30 μM Ba^{2+} was added in order to induce time-dependent current decay, allowing for nonstationary fluctuation analysis to be used for unitary current estimates (see below).

For some experiments, recording solutions also contained 100 mM *N*-methyl-D-glucamine chloride (NMG^+Cl^-) to "screen" charges. In some studies, transfected cells were pretreated in our culture medium (see below) for 5 min with 50 mM trimethyloxonium (TMO), an agent used to esterify carboxylic acid residues of negatively charged amino acid side chains (Sigworth and Spalding, 1980; Dudley and Baumgarten, 1993). To replace negative charges in some studies using mutant channels, 1 mM MTSES (in DMSO) was added for 10–15 min and then thoroughly washed out with fresh bath solution before recording. TW140F-4 patch pipettes (World Precision Instruments) were pulled and fire polished to give resistances of 6–10 MΩ for single channel recordings and resistances 2 MΩ for fluctuation analysis recordings. Pipettes were coated with Sylgard (Dow Corning Corporation) to reduce their capacitance. Data were acquired using Axopatch 200A amplifier, collected at 20 kHz by Clampex 8 (pCLAMP; Axon Instruments) with a 2 kHz low-pass Bessel filter and analyzed using Clampfit 8 (pCLAMP; Axon Instruments).

To obtain estimates for the unitary conductance (γ) at varied levels of symmetric K^+ in our cell attached recordings, it is desirable for the K^+ concentrations to equilibrate across the cell membrane and for the resting membrane potential to be 0 mV. For thermodynamic reasons, this cannot be readily established directly from our cell-attached recordings. Therefore, to demonstrate K^+ ion equilibration, we used the voltage-sensitive dye *bis*-(1,3-dibutylbarbituric acid)pentamethine oxonol ($DiBAC_4(5)$) (Molecular Probes), which increases its fluorescence as the membrane potential depolarizes. To perform these studies, $DiBAC_4(5)$ was dissolved in 0.2% DMSO and added to bath solutions at a final concentration of 200 nM. Initially transfected cells were incubated for 20 min with a solution containing 140 mM KCl, 10 mM HEPES, 2 mM $MgCl_2$, 200 nM $DiBAC_4(5)$, pH 7.4. Next, the fluorescence (at 616 nm) generated by $DiBAC_4(5)$ illuminated at 590 nm was recorded every 3 s from cells expressing Kir2.1 channels, identified by GFP fluorescence. Fig. 1 shows typical fluorescence recordings from $DiBAC_4(5)$ in response to changes in K^+ levels from 140 mM to 20 mM K^+ (20 mM K^+, 10 mM HEPES, 220 mM glucose, 2 mM $MgCl_2$, 200 nM $DiBAC_4(5)$, pH 7.4). As expected from the properties of $DiBAC_4(5)$, the application of 20 mM K^+ results in rapid fluorescence decreases, indicative of membrane hyperpolarization, which was followed by a slow return of the fluorescence to baseline, recorded when 140 mM K^+ was present. Furthermore, reintroduction of a 140 mM K^+ containing solution, caused a rapid increase in fluorescence, indicating membrane depolarization followed again by decay back to baseline. Identical patterns of $DiBAC_4(5)$ fluorescence changes were observed when other solution changes were applied. In general, these observations can only be obtained if K^+ ions equilibrate and have equal concentrations across the cell membrane. This conclusion is bolstered by the reasonable assumption that the initial membrane potential in our 140 mM K^+

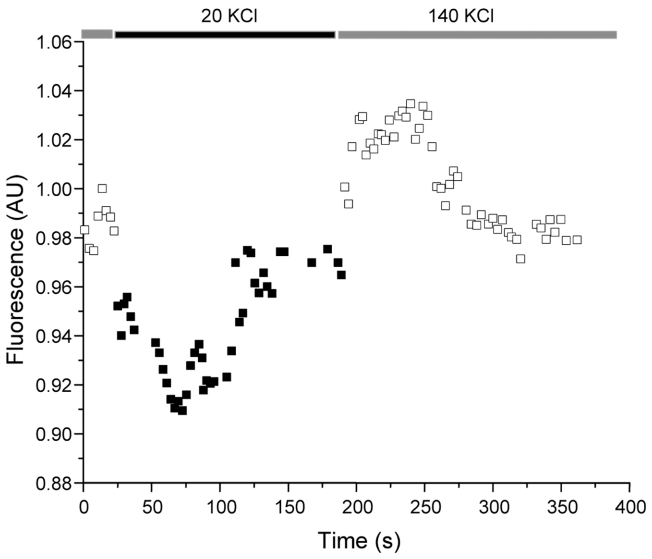

FIGURE 1. Fluorescence measurements of membrane potential using the voltage-sensitive dye $DiBAC_4(5)$. Baseline $DiBAC_4(5)$ fluorescence after 20 min of equilibration with a 140 mM K^+-containing solution (approximately equal to the intracellular concentration of K^+ of all mammalian cells) is shown followed by the changes in $DiBAC_4(5)$ fluorescence following the application of a 20 mM K^+ solution (■). Notice that the fluorescence initially decreases, indicative of an expected hyperpolarization following the application of 20 mM K^+. This is followed by a slow return to baseline over a 2-min period, indicative of a return to a membrane potential of 0 mV. When a 140 mM K^+ solution (□) is reapplied, an increase in fluorescence is observed, consistent with a membrane depolarization, which again is followed by a return to the baseline fluorescence. These results establish that K^+ levels equilibrate in our cells and that the membrane potential is zero within 2–3 min following changes in the applied K^+ concentrations.

containing solution was 0 mV (since intracellular environment of our cells should be typical of other mammalian cells that contain ~140 mM K^+), thereby indicating that the baseline fluorescence in our recordings corresponds to a membrane potential of 0 mV.

The observation that the membrane potential equilibrates to 0 mV and the K^+ levels are equal across the cell membrane (regardless of the applied external K^+ level) is entirely expected for the following reasons. First, the conductance of these cells following transfection is very high (i.e., >40 nS) and K^+ selective, which promotes K^+ equilibration across the membrane. Second, since Na^+ was excluded from the media, thereby inhibiting the Na^+ pump, there is no biochemical mechanism (that we are aware of) to maintain K^+ gradients across the membrane.

Nonstationary Fluctuation Analysis (NSFA) on Cell-attached Multichannel Recordings

Unitary currents were estimated by the nonstationary fluctuation analysis (NSFA) method using the equation (Sigworth, 1980)

$$\sigma^2 = -\frac{1}{N}\langle I\rangle^2 + i\langle I\rangle + L, \quad (1)$$

where σ^2 is the variance of the measured macroscopic current, I, $\langle I\rangle$ is the mean of I, N is the number of channels in the patch, and L is the contribution of leak currents. Since Kir2.1 channels do not vary greatly in response to voltage steps as is required for NSFA, Ba^{2+} was included in the extracellular solutions to induce time- and voltage-dependent block of Kir2.1 currents (Neyton and Miller, 1988; Jiang and MacKinnon, 2000). In the presence of Ba^{2+}, 200–300 successive K^+ current sweeps were recorded in response to voltage steps from a holding potential of +5 mV to −60, −80, −100, −120, and −140 mV. Variance and mean currents were estimated using consecutive pairs of traces (to minimize the complicating effects of current drift) and these estimates for σ^2 and $\langle I\rangle$ were averaged. Estimates for σ^2 versus $\langle I\rangle$ were fit with Eq. 1 using Maple 7.00 (Waterloo Maple Inc.) to estimate *i*. The single-channel conductance (γ) was calculated from the dependence of unitary current estimates on voltage using Ohm's law (Kubo et al., 1993; Fig. 2 B).

Unitary Conductance–K^+ Activity Relationship

To properly account for the effect of counter-ions in the solution on the driving force for K^+ ion entry into the pore (i.e., the chemical potential), the activity of K^+ (a_K) was calculated using the relationship

$$a_K = f_K^{act}[K^+]. \quad (2)$$

To accurately estimate the contribution of long-range electrostatic interactions to the activity coefficients, f_K^{act}, in our studies we used the following equations. When the ionic strength (I) was <10 mM (i.e., $I < 10$ mM), f_K^{act} was calculated using the relationship (Debye and Hückel, 1923)

$$\log_{10} f_K^{act} = (-0.509)|z_+ z_-|\sqrt{I}, \quad (3)$$

where z_+ is the valence of the major cation, z_- the major anion, and I is the ionic strength of the solution, which is defined as (Debye and Hückel, 1923)

$$I = \frac{1}{2}\sum_{i=1}^{n} c_i z_i^2. \quad (4)$$

For 10 mM < I < 100 mM, the Extended Debye-Hückel relationship was used (Kielland, 1937; MacInnes, 1961):

$$\log_{10} f_K^{act} = (-0.509)|z_+ z_-|\left(\frac{\sqrt{I}}{1 + Ba\sqrt{I}}\right), \quad (5)$$

where $B \approx 0.33$ in water at 25°C and a is an adjustable parameter corresponding to ionic size ($=3 \times 10^{-8}$ cm for K^+). For $I > 100$ mM, we used Davies' approximation (MacInnes, 1961),

$$\log_{10} f_K^{act} = (-0.509)|z_+ z_-|\left(\frac{\sqrt{I}}{1 + \sqrt{I}} - 0.3I\right), \quad (6)$$

The dependence of γ on a_K (i.e., the γ–a_K relationship) was initially fit with a modified Langmuir binding isotherm (Fig. 3 B):

$$\gamma = \frac{\gamma_{max} a_K}{EC_{50} + a_K} + S, \quad (7)$$

where a_K is defined by Eq. 3, 5, or 6 as required, γ_{max} is the maximal conductance measured at saturating a_K, and EC_{50} is a measure of a_K when γ is $\gamma_{max}/2$. The parameter S is required to account for the nonzero intercept of the γ–a_K relationship which is predicted to originate from the presence of surface charges (see below).

Surface Charge Calculations

To quantify the contribution of surface charges to Kir2.1 channel properties, we assumed that the conductance is a function of the

activity of K^+ ions at the channel surface (a_K^s) and not a_K in the bulk solution. a_K^s was estimated by the relationship

$$a_K^s = a_K \exp\left(\frac{-ze\phi_s}{k_B T}\right), \quad (8)$$

where z, e, k_B, and T have their usual meanings, and ϕ_s is the electrostatic potential at the surface. In our studies, we estimated ϕ_s using the relationship (McLaughlin et al., 1970)

$$\phi_s = -\frac{k_B T}{ze} \ln \frac{\gamma_{control}}{\gamma_{TMO}}, \quad (9)$$

where $\gamma_{control}$ is the channel conductance in the presence of surface charges, and γ_{TMO} is the unitary conductance in following pretreatment with TMO that was assumed to neutralize all negative surface charges. Evidence for the validity of this assumption is provided in the results section.

To estimate the number of charged residues that might contribute to the observed surface charge effects, the surface charge density (σ) was calculated using the following equation (Grahame, 1947; McLaughlin, 1977):

$$\sigma = \left[\sinh\left(\frac{ze\phi_s}{2k_B T}\right)\right][8\varepsilon_r\varepsilon_o RT a_K]^{1/2}\left[1 + a_a a_K \exp\left(\frac{-ze\phi_s}{k_B T}\right)\right], \quad (10)$$

where $a_a = 0.15\ M^{-1}$ (Eisenberg et al., 1979), a_K is the activity in the bulk solution, ε_r is assumed to be the dielectric of water (80), and ε_o is the permittivity of free space. Values of σ for every ϕ_s and a_K^s were averaged (±SEM) to determine the final estimate.

Kinetics of Barium Block

Since Ba^{2+} blocks Kir2.1 channels by binding within the selectivity filter, time constants (τ) for Kir2.1 current decay in the presence of Ba^{2+} are predicted to be influenced by surface charges in a manner similar to K^+ conductance (see above). By assuming that Ba^{2+} block is adequately described by a single binding site model (Neyton and Miller, 1988; Alagem et al., 2001) where only the on-rate is influenced by the surface potential combined with the assumptions that the rate of Ba^{2+} entry into the channel is given by the Ba^{2+} activity at the channel surface (a_{Ba}^s) and that Ba^{2+} does not alter the surface potential at the low concentrations used (see Eqs. 3 and 4), we can write

$$\frac{1}{\tau}(V) = k_{on}(V) a_{Ba}^s + k_{off}(V), \quad (11)$$

where $k_{on}(V)$ and $k_{off}(V)$ are the rates of Ba^{2+} binding and unbinding, respectively, at a given voltage, and a_{Ba}^s is the external Ba^{2+} activity at the surface of the channel, which is related to Ba^{2+} activity in the bulk (a_{Ba}) as described above for K^+ ions in Eq. 6. Assuming that $k_{on}(V)$ depends exponentially on voltage (Reuveny et al., 1996), it can be shown that

$$\ln\left[\Delta\left(\frac{1}{\tau}(V)\right)\right] = \ln\left[k_{on}(0) a_{Ba}\left(\exp\left(\frac{ze\phi_s}{k_B T}\right) - 1\right)\right] - \frac{ze\delta_{on}}{k_B T} V, \quad (12)$$

where $\Delta(1/\tau)$ is the difference in $1/\tau$ for a given $[Ba^{2+}]$ in the presence and absence of NMG, and δ_{on} is an estimate of the electrical distance for the position of the peak of the free energy barrier for Ba^{2+} binding to the channel pore. $k_{on}(0)$ and δ_{on} were obtained from the intercept and slope of the relationship between $1/\tau$ and voltage (−80, −100, and −120 mV) in the presence of NMG (i.e., where the surface charges are screened) (Reuveny et al., 1996). Estimates of ϕ_s using this method were made at each voltage and averaged in order to determine σ_{Ba}.

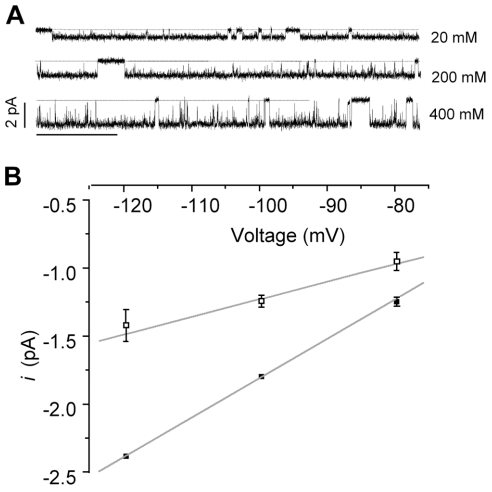

FIGURE 2. Single channel measurements of Kir2.1 unitary currents at various $[K^+]$. (A) Representative traces recorded at −120 mV in symmetrical K^+ concentrations of 20, 200, and 400 mM. The solid lines represent the zero current level (channel closed). It becomes increasingly difficult to distinguish single channel openings as $[K^+]$ approaches 0 mM. (B) Unitary currents recorded with symmetrical 20 mM (□) and 140 mM (■) K^+ show the ohmic behavior (solid line) of Kir2.1 currents between −80 and −120 mV.

Data Analysis

With the exception of NSFA, all other data were analyzed using Origin 6.0 (Microcal Software Inc.). This includes mathematical calculations, graph development, curve fitting with the appropriate functions, as well as statistical analysis.

RESULTS

Kir2.1 Single-channel Conductances at Varying K^+ Concentrations

To investigate the existence of surface charges in Kir2.1 channels, we examined the conductance as a function of K^+ activity. Fig. 2 A illustrates typical single channel currents (*i*) recorded in CHO cells transfected with Kir2.1 channels at several K^+ concentrations. As shown in Fig. 2 B for 20 and 140 mM K^+, *i* depends linearly on voltage (i.e., the channels are ohmic) over the range of voltages studied as previously reported (Kubo et al., 1993). Thus, unitary conductances (γ) were estimated using Ohm's Law. Since the unitary current could not be reliably measured using single-channel recordings with <20 mM K^+ for Kir2.1 channels, NSFA of currents recorded in cell-attached patches containing Ba^{2+} were used to estimate *i*. Typical cell-attached recordings are shown in Fig. 3 A, along with a typical plot of the mean variance ($<\sigma^2>$) versus mean current ($<I>$) assessed from analysis of 200 sweeps, which allowed estimates of *i* from the parabolic function in Eq. 1. Fig. 3 B plots the estimated unitary conductance from single channel recordings (closed squares) and NSFA (open squares) as a function of the bulk K^+ activity. Note that the γ esti-

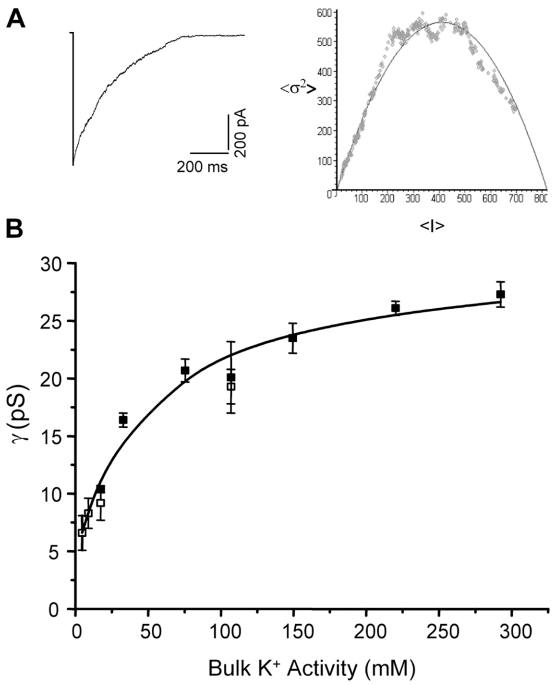

FIGURE 3. Unitary conductance (γ) estimates by single-channel recordings and nonstationary fluctuation analysis (NSFA). (A) Left, time- and voltage-dependent block is observed in a representative raw trace of macroscopic current decay from a cell-attached patch expressing Kir2.1 channels with 30 μM Ba^{2+} in the pipette allowing steps to −140 mV from a holding potential of +5 mV. Right, NSFA was performed on >200 of these sweeps by generating a mean variance (σ^2) versus mean current <I> plot, which was fit to the parabolic function in Eq. 1. (B) Plot of the unitary conductance (γ) as a function of symmetrical K^+ activity. Single-channel estimates are represented by closed squares (■), and estimates of γ from NSFA are shown in open squares (□). The solid line represents the fit to the modified Langmuir binding isotherm in Eq. 7.

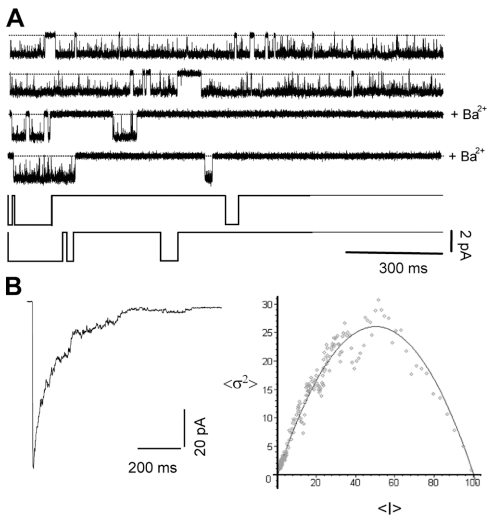

FIGURE 4. Monte Carlo simulations and validation of the NSFA method. (A) Raw traces (top four) of single channel openings in the absence (top two traces) or presence (middle two traces) of 30 μM Ba^{2+} in 140 mM K^+ at −140 mV. The mean open (52 ms) and closed times (78 ms) were used to estimate rate constants for Ba^{2+} binding (545.9 $ms^{-1} \cdot M^{-1}$) and unbinding (3.410^{-5} ms^{-1}), which were used in Monte Carlo simulations of Kir2.1 channels (bottom two traces). (B) Left, summation of 100 simulated single channel traces (bottom two traces in A) were used to construct macroscopic Ba^{2+}-blocked current. Right, 200 of the macroscopic currents were used to plot the mean variance versus mean current graph. Estimates of i (and therefore γ) obtained using NSFA were identical to input values, thus proving the validity of using this technique.

mates using NSFA were identical ($P < 0.01$) to the values estimated using single-channel recordings (at 20 and 140 mM K^+). These data were fit ($R^2 = 0.98$) using the modified Langmuir binding isotherm (see MATERIALS AND METHODS) to estimate γ_{max} (26.0 ± 1.5 pS, $10 < n < 20$) and EC_{50} (50 ± 15 mM a_K) as well as the intercept, S (4.4 ± 1.4 pS). These results establish a clear saturation of unitary conductance at high K^+ concentrations as reported previously (Stampe et al., 1998) and suggest the existence of a surface charge.

To ensure that our conductance estimates did not arise from experimental limitations of the NSFA method, we performed Monte Carlo simulations of channel blocking events (Hanna et al., 1996) using experimentally derived mean blocking and unblocking times in the presence of 30 μM Ba^{2+} (Table I) assuming a single site blocking model, as established previously (Neyton and Miller, 1988; Alagem et al., 2001). Typical simulated single-channel events are shown in Fig. 4 A (bottom two traces), while Fig. 4 B shows the predicted macroscopic current

TABLE I

Experimentally Determined Rate Constant Parameters

	with 30 μM Ba^{2+}		no Ba^{2+}			
Vm	k_{off}	k_{on}	mean open time	α	mean closed time	β
mV	ms^{-1}	$ms^{-1} \cdot M^{-1}$	*ms*	ms^{-1}	*ms*	ms^{-1}
−100	1.86×10^{-4}	135.6	70	0.0143	30	0.0333
−120	2.07×10^{-4}	309.9	70	0.0143	55	0.0182
−140	3.41×10^{-5}	545.9	52	0.0192	78	0.0128

Experimentally determined rate constant parameters (k_{on}, k_{off}, mean open, and mean closed times) for simulation of Kir2.1 single channel opening with 30 μM Ba^{2+}.

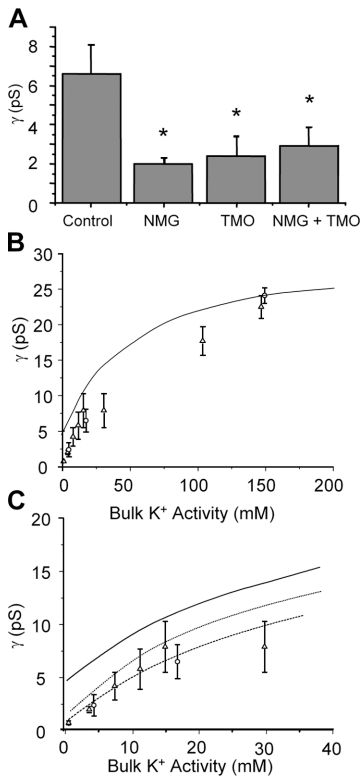

FIGURE 5. The effect of screening surface charges by NMG and TMO on γ at low K^+. (A) Comparison of γ at 5 mM K^+ in the absence of charge screening agents (control), in the presence of 100 mM NMG, pretreatment with 50 mM TMO, and pretreatment with TMO plus the addition of 100 mM NMG to the pipette solution. $P < 0.001$. (B) The presence of 100 mM NMG (Δ) or pretreatment with 50 mM TMO (○) to screen surface charge reduces γ at low K^+ activity, and eliminates the nonzero intercept at 0 mM K^+ ($10 < n < 20$). The solid black line represents best fit line for control data. (C) Expansion of 0–40 mM region in B. Dashed lines are fits of NMG and TMO data with the modified Langmuir binding isotherm.

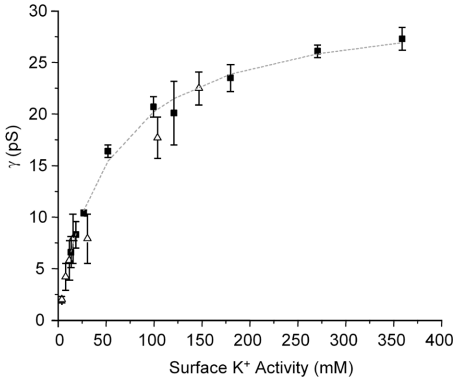

FIGURE 6. The relationship of conductance to K^+ activity at the channel surface. The γ–a_K^s relationship, which accounts for the effects of surface charges, in control conditions (■) can be well described ($R^2 = 0.99$) by a Langmuir binding isotherm (dashed line) going through the origin (0.7 ± 1.5 pS, $P = 0.36$). γ–a_K^s estimates for channels in the presence of NMG (Δ) fall on the same curve, indicating that surface charges alone can account for the shift in local ion activity and the increased conductance through Kir2.1 channels that result.

generated by superimposing 100 sweeps, as well as the predicted dependence of $<\sigma^2>$ on $<I>$. Clearly, the simulated results in Fig. 4 B (left) closely resemble the experimental results in Fig. 3 A. More important, the estimated unitary current estimated from the $<\sigma^2>$ versus $<I>$ plot is identical to the assumed unitary current (Makhina et al., 1994, Krapivinsky et al., 1998).

Charge Screening Decreases Kir2.1 Single Channel Conductance at a Low K^+

The presence of the nonzero intercept, S, in the γ versus a_K relationship suggests the presence of a surface charge. To investigate this possibility, the γ versus a_K relationship was measured in the presence of 100 mM NMG to screen surface charges. As shown in Fig. 5 B, with 200 mM symmetrical K^+ (see MATERIALS AND METHODS), the inclusion of 100 mM NMG did not affect the Kir2.1 single channel conductance (solid line is without NMG), confirming that NMG does not block Kir2.1 channels. By contrast, at 5 mM K^+, the single channel conductance was reduced ($P < 0.01$) to 2.0 ± 0.3 pS in the presence of 100 mM NMG compared with 6.6 ± 1.5 pS in the absence of NMG (Fig. 5 A). Reductions in γ were also observed at 10, 15, 20, and 40 mM K^+, when 100 mM NMG was added ($P < 0.05$). More important, fitting the γ–K^+ activity relationship with Eq. 7, when 100 mM NMG was present, reduced the conductance intercept to a value not different from zero (i.e., 0.8 ± 1.3, $P = 0.36$) (Fig. 5 C).

As an alternate method for eliminating surface charges, CHO cells were treated with TMO, a carboxylate esterifying agent. The unitary conductance with TMO was 2.4 ± 1.0 pS with 5 mM K^+ which was below ($P < 0.01$) the value of γ estimated without TMO treatment (Fig. 5 A). Furthermore, the unitary conductance in 5 mM K^+ after treatment with TMO was not reduced further by the inclusion of 100 mM NMG (2.9 ± 1.0 pS) (Fig. 5 A), and the intercept for the γ versus a_K relationship (0.8 ± 1.9 pS) was not different ($P = 0.32$) from zero. Taken together, these results suggest that negatively charged amino acid residues generate surface charges in Kir2.1 channels, thereby increasing unitary currents at low permeant ion concentrations.

Electrostatic Theory Predictions of Surface Charge Effects

Using our results above, it is possible to calculate the surface charge potential (ϕ_s) for Kir2.1 channels (Eq. 9) and thereby the activity of K^+ ions at the mouth of the channel pore (i.e., a_K^s) (using Eqs. 8 and 9). Fig. 6 shows the relationship between γ and a_K^S (closed squares), which can be well fit ($R^2 = 0.99$) with Eq. 7 going through the origin ($S = 0.7 \pm 1.5$ pS, $P > 0.05$).

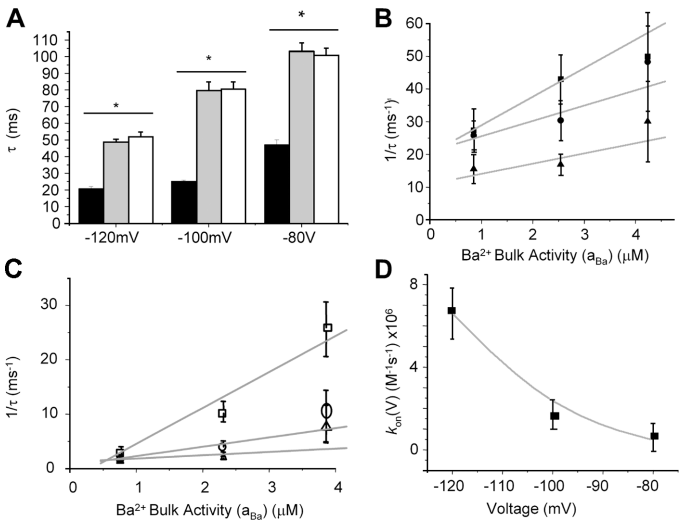

FIGURE 7. Barium blocking kinetics under various experimental conditions. (A) Blocking time constants (τ) estimated after pretreating with 50 mM TMO (gray) or in the presence of 100 mM NMG (white) compared with control data (black) at 5 mM K^+. (B) The relationship between $1/\tau$ versus Ba^{2+} activity in the presence of 20 mM K^+ at −80 mV (▲), −100 mV (●), and −120 mV (■). (C) The relationship between $1/\tau$ versus Ba^{2+} activity in the presence of 20 mM K^+ plus 100 mM NMG at −80 mV (△), −100 mV (○), and −120 mV (□). (D) The slopes calculated in C were used to determine $k_{on}(V)$ (■) and plotted versus voltage to estimate $k_{on}(0)$ and δ_{on} (Reuveny et al., 1996), which were in turn used to determine an apparent charge density (σ_{Ba}) of -0.49 ± 0.12 e nm^{-2} on the surface of Kir2.1 channels, in line with estimates from our conductance data.

Notice that the relationship of γ versus a_K^s in control conditions is identical to the γ versus a_K (i.e., bulk K^+ activity) relationship for channels in the presence of NMG (open triangles), consistent with a role for surface charges in concentrating permeant K^+ ions at the channel surface.

Our estimates of ϕ_s were also used to calculate the apparent surface charge density (σ) of Kir2.1 channels (Eq. 10). Values of charge density in Kir2.1 channels were calculated for each a_K^s examined assuming a dielectric (ε_r) of 80 (that of water), and then averaged to determine a σ of -0.49 ± 0.08 e nm^{-2}. When NMG was present, the estimated surface charge was reduced to -0.06 ± 0.02 e nm^{-2}, which represents less than one net charge per channel subunit. This is consistent with the screening of surface charges in Kir2.1 channels by NMG. Using current molecular models of Kir2.1 channels (Cho et al., 2000), we estimated the channel's surface area to be ~11 nm^2, which predicted the presence of approximately −5.4 e net charges per channel. Since Kir2.1 channels are tetramers, these calculations suggest that the surface charge arises from one free net charge per monomer.

Kinetics of Extracellular Barium Block Are Altered by Charge Screening

Ba^{2+} is a potent voltage- and time-dependent blocker of K^+ current in Kir2.1, by binding within the selectivity filter (Jiang and MacKinnon, 2000). Thus, the presence of surface charges is predicted to alter the blocking time constant (τ) of Ba^{2+}. Indeed, as shown in Fig. 7 A, treatment with NMG or TMO significantly increased τ at 5 mM K^+ compared with control. The same was observed for 20 mM (Fig. 7, compare B and C) and 140 mM [K^+]. Using the voltage dependence of k_{on} in the absence of surface charges (Fig. 7 D) and Eqs. 11 and 12, ϕ_s was calculated using Ba^{2+} blocking kinetics for 20 mM K^+, which again allows an estimate of the charge density (σ_{Ba}) in Kir2.1. σ_{Ba} was estimated to be -0.49 ± 0.12 e nm^{-2}, which is indistinguishable ($P < 0.01$) from the value obtained using the conductance data, confirming the presence of four negative charges on the surface of Kir2.1 channels.

Identification of Extracellular Charges Acting as Surface Charges

Using the molecular model for Kir2.1 channels, which is based on the *KcsA* crystal structure (Cho et al., 2000), we identified three candidate charged residues (E125, D152, and E153) that might act as surface charges (Fig. 8 A). We replaced these charged residues with cysteine in order to examine the potential role of these charges in the electrostatic effects of Kir2.1 channels. Cysteine was chosen to allow charge replacement using MTS compounds. The dependence of γ on a_K was unaltered for E125C and D152C mutant channels, compared with wild-type (WT) channels at 20 mM K^+ (Fig. 8 B). On the other hand, E153C channels showed a smaller unitary conductance compared with WT, which was not different from the unitary conductance observed in WT channels pretreated with TMO (Fig. 8 B) ($P < 0.01$). Fig. 8 C shows that the same results were observed for 5 mM K^+, whereas, at 140 mM K^+, WT channels, with and without TMO treatment, and all three mutant channels had similar γ values. Treatment of E153C channels with MTSES, in order to replace the negative charge, increased the γ to levels similar to WT at 20 mM K^+ (Fig. 8 B). Taken together, these results support the conclusion that E153 acts as the primary source of surface charges in Kir2.1 channels.

DISCUSSION

Our results establish that Kir2.1 channels display classical surface charge properties (Sigworth and Spalding, 1980;

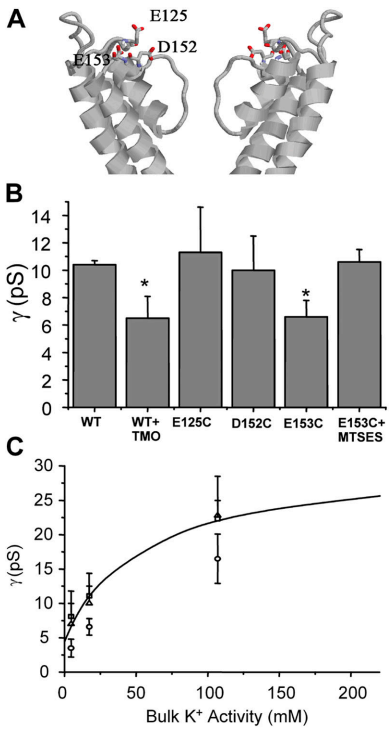

FIGURE 8. The contribution of putative negatively charged extracellular residues. (A) The top portion of A and C monomers of the Kir2.1 channels from recent molecular models (Cho et al., 2000) to illustrate the location of E125, D152, and E153 negatively charged residues and emphasizing their proximity to the pore mouth of the channel. (B) A comparison of γ values in WT (control and pretreated with 50 mM TMO), E125C, D152C, and E153C mutant channels at 20 mM K^+ shows there is a significant reduction in unitary conductance in E153C channels compared with WT, and that this reduction is indistinguishable from that caused by pretreatment with TMO. Charge replacement by MTSES for E153C channels returns unitary currents to WT levels. ($P < 0.001$). (C) Kir2.1 single-channel conductance (γ) as a function of symmetrical K^+ activity in the absence of surface charge screening agents. E125C (□) and D152C (Δ) mutant channels have γ that are indistinguishable from WT Kir2.1 channels' data (solid black line). E153C mutant channels (○) have reduced γ–K^+ activity relationships compared with WT channels ($7 < n < 20$).

Worley et al., 1986; MacKinnon and Miller, 1989; MacKinnon et al., 1989) that depend on E153 residues predicted from a previous molecular model to be located on the outer face of the channel (Cho et al., 2000). Investigations into the possible role of surface charges in our studies necessitated the conversion of K^+ ion concentrations into chemical activity (i.e., chemical potential) in order to account for the effects of ionic strength on the thermodynamic driving force of K^+ ions into Kir2.1 channels. K^+ activity was calculated using a combination of the linear Debye-Huckel, the Extended Debye-Huckel, and the Davies' theories to account for long-range electrostatic interactions between ions in solution under our experimental conditions (Debye and Hückel, 1923; MacInnes, 1961). The use of multiple equations was necessary because no single analytical expression can comprehensively estimate ionic activities over the range of experimental conditions used in our studies (MacInnes, 1961). The use of K^+ activity was essential in our studies since a wide range of ionic strengths were used to alter surface potentials in Kir2.1 channels.

In our studies, it was necessary to determine the unitary current and unitary conductance (γ) with varied symmetric levels of K^+. This could not be achieved using whole-cell recordings since the current magnitudes were too large to allow NSFA to be effectively used (see below). Therefore, to circumvent this problem, we resorted to cell-attached recordings. To ensure the levels of K^+ were symmetric in our cell-attached recordings, we monitored the membrane potential using a voltage-sensitive dye. These studies showed that K^+ levels equilibrate within 2–3 min following changes of the external K^+ levels under our experimental conditions, probably due to the presence of very high levels of Kir2.1 channel expression (i.e., >40 nS in whole-cell recordings with 140 mM K^+) combined with the omission of Na^+, thereby inhibiting the Na^+ pump.

Clear evidence for the presence of surface charges was obtained in our studies using two methods that yielded comparable estimates for the electrostatic surface potential in Kir2.1 channels. In the first method, the dependence of unitary current (γ) on the K^+ activity was used. These studies required the use of NSFA at low K^+ activities, due to small unitary currents, as done previously in HRK1 (Makhina et al., 1994) and Kir7.1 (Krapivinsky et al., 1998) channels. We validated the NSFA method in our studies using Monte Carlo simulations to model Ba^{2+} blocking events. In the γ versus a_K plots, we found that γ does not approach zero as K^+ activities are reduced. While it is possible that the finite limiting γ intercept originates from finite permeability of Kir2.1 channels to other cations in our solutions (e.g., Ba^{2+}), Kir2.1 channels are impermeant to these other ions (Alagem et al., 2001). More important, the limiting γ was reduced to zero at low a_K following the addition of the impermanent cations NMG^+ to screen surface charges or following pretreatment of the channels with TMO to specifically neutralize carboxylate residues (Parsons et al., 1969; Nakayama et al., 1970). The nonzero conductance intercept at low K^+ activity, combined with a zero conductance intercept at high ionic strength or following TMO pretreatment are signature features of local surface charges (Manning, 1978; Fixman, 1979; Klein et al., 1981; Cai and Jordan, 1990).

To analyze and interpret our γ versus a_K results we used the Gouy-Chapman-Stern (GCS) theory for surface charges, which assumes the surface charge density is uniformly distributed in a flat plane. While this assumption is generally expected to be invalid for ion

channel proteins, the GCS theory accurately accounts for surface charge effects in many proteins, possibly due to cancellation of errors in the functional expansions of rigorously correct canonical partition functions (Fixman, 1979; Klein et al., 1981). We anticipate that the applicability of the GCS theory is assisted by the symmetrical arrangement of four negative point charges around the pore opening of tetrameric Kir2.1 channels that should mimic more closely a uniform charge distribution than a single point charge located near the pore opening. Regardless, the application of the GCS theory to our results predicted that γ depends uniquely on the local K^+ ion activity at the entrance to the Kir2.1 channel pore. Indeed, the dependence of γ on a_K at the channel surface (i.e., a_K^s) could be accurately described by a Langmuir binding isotherm going through the origin. The GCS theory further predicted a surface charge density of -0.49 ± 0.08 e nm^{-2}. Using recent molecular models of Kir2.1 channels (Cho et al., 2000) to estimate channel area, we calculated a net of approximately four charges on the surface of Kir2.1 channels in the absence of charge screening agents, which equated to nearly one charge per monomer.

Thus, our γ results strongly support the conclusion that surface charges influence the Kir2.1 channel conductance. Similar investigations and analyses have been applied to other channels, including Na^+ channels (Sigworth and Spalding, 1980; Worley et al., 1986), Ca^{2+}-activated K^+ channel (Moczydlowski et al., 1985; MacKinnon and Miller, 1989; MacKinnon et al., 1989; Park et al., 2003), NAChRs (Imoto et al., 1988; Konno et al., 1991), to establish the presence of surface charges. On the other hand, γ versus concentration in *KcsA* channels show two asymptotic conductance values at low and high K^+ levels (Morais-Cabral et al., 2001; Nimigean et al., 2003). The limiting γ value of *KcsA* at low K^+ levels appears remarkably similar to that observed in Kir2.1 channels, suggesting that surface charges may also play an important role in the conductance properties of these channels as well.

Since Ba^{2+} blocks Kir2.1 channels by binding within the channel pore, Ba^{2+} should be affected by the presence of surface charges in a comparable manner to K^+ ions. Specifically, the rate of Ba^{2+} entry into the channel should be proportional to the activity of Ba^{2+} at the channel entry. This provided a second method for estimating surface charges in Kir2.1. Indeed, when charges are screened by NMG, or neutralized by TMO, the kinetics of Ba^{2+} block is slowed significantly. Furthermore, after accounting for ionic strength (i.e., activity) of Ba^{2+} in our recording conditions, our estimates of the surface charge density from our Ba^{2+} block studies (σ_{Ba}), using the GCS theory, were identical to those estimated from our conductance studies, once again supporting the existence of four negative charges on the surface of Kir2.1 channel proteins. This contrasts with a previous report examining the effects of lipid charges on BK channels (Park et al., 2003), where alterations in lipid charge (i.e., lipid surface charges) affected BK channel conductance, but not Ba^{2+} block properties. This led the authors to conclude, consistent with molecular models of channel proteins, that lipid charges are too remote from the channel pore entrance to produce classical surface charge effects (Park et al., 2003). While we did not examine the effects of altered lipid composition on the Kir2.1 channel properties, our results are consistent with the conclusions of Park et al. (2003) since surface charge effects in Kir2.1 channels originate from charged E153 (see below), predicted to be more adjacent to the channel pore entrance than charged lipids. Further studies will be required to examine whether lipid charge also affects Kir2.1 channel properties.

More definitive evidence for the existence of surface charges in Kir2.1 channels was provided by our mutagenesis studies. Somewhat surprisingly, E125C and D152C mutant channels showed conductance properties identical to WT channels. Previous studies have suggested that E125 contributes a superficial site for binding of extracellular divalent cations such as Mg^{2+}, Ba^{2+}, and Ca^{2+} (Murata et al., 2002). Indeed, in the presence of divalents, E125Q mutant channels had decreased single-channel conductance compared with WT channels. Furthermore, the E125 was also postulated to play a key role in dehydration of Ba^{2+} before entering the pore (Alagem et al., 2001). Consistent with these results, Ba^{2+} blocking kinetics were increased in E125C mutant channels compared with WT channels. The significance of these observations is unclear but could arise from altered binding affinities for these divalents at this site.

Our observations in D152C channels were unexpected, based on our model of Kir2.1 channels (Cho et al., 2000). This may indicate that the D152 residue binds K^+ ions with high affinity, thereby not contributing to the surface charge effect. Alternatively, our molecular model (Cho et al., 2000) may require revision with the D152 residue either buried or oriented in such a way that its side chain does not contribute to the surface potential. Although less likely, it is conceivable that the sulfhydryl side chains of the C125 and C152 residues may be ionized in the E125C and D152C mutant channels. Consequently, the residues would not have led to charge neutralization, thereby having maintained their surface potential. However, this possibility would be inconsistent with the expectation that polar residues are less likely (not more likely) to be ionized (i.e., have a higher pKa) when localized in regions with reduced dielectric constants, such as in proteins compared with the aqueous phase.

Unlike E125C and D152C mutant channels, E153C channels have reduced single-channel conductance

compared with WT channels at low ionic activities and are identical in conductance properties to WT channels pretreated with 50 mM TMO (Fig. 8 B). Moreover, addition of 1 mM MTSES to restore negative charges restored WT behavior to E153C channels (Fig. 8 B). These results support the conclusion that E153 is responsible for the surface charge effects observed in Kir2.1 channels by contributing approximately one negative charge per monomer at the channel surface. In accordance with electrostatic theory, our results support the conclusion that ionized carboxyl groups increase the conduction at low permeant ion activities, by attracting the permeant ions near the conduction pathway.

Our results also establish that for Kir2.1 channels, γ increases with elevations in a_K, exhibiting a clear maximum conductance >160 mM (K^+ concentrations >300 mM) with an apparent a_K EC_{50} of 50 ± 15 mM. These properties of Kir2.1 channels resemble those of ROMK1 (Kir1.1) channels that have a similar EC_{50}, although ROMK1 channels exhibit a maximum conductance as a_K is elevated above 300 mM K^+ (Heginbotham and MacKinnon, 1993; Lu and MacKinnon, 1994). It is conceivable that γ of Kir2.1 channels might also reach a maximum at higher K^+ concentrations. In stark contrast to Kir1.1 and Kir2.1 channels, the γ–[K^+] relationship in *KcsA* channels is nearly linear from 50 to 500 mM K^+ (Morais-Cabral et al., 2001), with evidence of saturation at K^+ concentrations >1600 mM K^+ (Nimigean et al., 2003). The basis for the differences in the γ properties of various inward rectifier channels will clearly require further investigations.

While our studies focused on the contribution of surface charges from E153 residues to Kir2.1 channel conductance, it is conceivable that surface charges may affect other channel properties. Indeed, since polyamine and Mg^{2+} block Kir2.1 channels by binding within the channel pore, alterations in surface charges could conceivably alter binding stability of these blockers. Thus, surface charge effects may contribute to the crossover effect observed in Kir2.1 channels with increased extracellular [K^+].

Our findings support the presence of approximately four negative charges on the surface of Kir2.1 channels, originating from E153 (but not E125 or D152) residues. The results of our studies should help guide the development of new molecular models of Kir2.1 channels in the absence of crystal structures. It is apparent that new models of Kir2.1 channels must reexamine the location, orientation, and ionization of these three residues to account for the surface charge effect we attribute to the E153 residue. As well, future studies of ion occupancy, permeation, and perhaps rectification in Kir2.1 channels need to consider surface charge effects as described in our studies.

We thank L.Y. Jan for providing us with the Kir2.1 clone and A. Prendergast for his technical assistance.

This study was supported by Heart and Stroke Foundation of Ontario (grant T-4179) to P.H. Backx. P.H. Backx is a Career Investigator of the Heart and Stroke Foundation of Ontario. H.C. Cho was supported by a Canadian Institutes of Health Research studentship. N. D'Avanzo holds a studentship from Heart & Stroke Richard Lewar Center of Excellence at the University of Toronto.

David C. Gadsby served as editor.

Submitted: 25 August 2004
Accepted: 18 March 2005

REFERENCES

Alagem, N., M. Dvir, and E. Reuveny. 2001. Mechanism of Ba^{2+} block of a mouse inwardly rectifying K^+ channel: differential contribution by two discrete residues. *J. Physiol.* 534:381–393.

Apell, H.J., E. Bamberg, H. Alpes, and P. Lauger. 1977. Formation of ion channels by a negatively charged analog of gramicidin A. *J. Membr. Biol.* 31:171–188.

Berneche, S., and B. Roux. 2001. Energetics of ion conduction through the K^+ channel. *Nature.* 414:73–77.

Berneche, S., and B. Roux. 2003. A microscopic view of ion conduction through the K^+ channel. *Proc. Natl. Acad. Sci. USA.* 100: 8644–8648.

Beuckelmann, D.J., M. Nabauer, and E. Erdmann. 1993. Alterations of K^+ currents in isolated human ventricular myocytes from patients with terminal heart failure. *Circ. Res.* 73:379–385.

Cai, M., and P.C. Jordan. 1990. How does vestibule surface charge affect ion conduction and toxin binding in a sodium channel. *Biophys. J.* 57:883–891.

Cho, H.C., R.G. Tsushima, T. Nguyen, H.R. Guy, and P.H. Backx. 2000. Two critical cysteine residues implicated in disulfide bond formation and proper folding of Kir2.1. *Biochemistry.* 39:4649–4657.

Debye, P., and E. Hückel. 1923. Zur Theorie der Elektrolyte. II. Das Grenzgesetz fur die elektrische Leitfahigkeit. *Physiol. Z.* 24:305–325.

Doyle, D.A., J.M. Cabral, R.A. Pfuetzner, A. Kuo, J.M. Gulbis, S.L. Cohen, B.T. Chait, and R. MacKinnon. 1998. The structure of the potassium channel: molecular basis of K^+ conduction and selectivity. *Science.* 280:69–77.

Dudley, S.C., Jr., and C.M. Baumgarten. 1993. Modification of cardiac sodium channels by carboxyl reagents. Trimethyloxonium and water-soluble carbodiimide. *J. Gen. Physiol.* 101:651–671.

Eisenberg, M., T. Gresalfi, T. Riccio, and S. McLaughlin. 1979. Adsorption of monovalent cations to bilayer membranes containing negative phospholipids. *Biochemistry.* 18:5213–5223.

Fixman, M. 1979. The Poisson-Boltzmann equation and its application to polyelectrolytes. *J. Chem. Physiol.* 70:4995–5005.

Getzoff, E.D., D.E. Cabelli, C.L. Fisher, H.E. Parge, M.S. Viezzoli, L. Banci, and R.A. Hallewell. 1992. Faster superoxide dismutase mutants designed by enhancing electrostatic guidance. *Nature.* 358:347–351.

Getzoff, E.D., J.A. Tainer, P.K. Weiner, P.A. Kollman, J.S. Richardson, and D.C. Richardson. 1983. Electrostatic recognition between superoxide and copper, zinc superoxide dismutase. *Nature.* 306:287–290.

Grahame, D.C. 1947. The electrical double layer and the theory of electrocapiliarity. *Chem. Rev.* 41:441–501.

Hanna, W.J., R.G. Tsushima, R. Sah, L.J. McCutcheon, E. Marban, and P.H. Backx. 1996. The equine periodic paralysis Na^+ channel mutation alters molecular transitions between the open and in-

activated states. *J. Physiol.* 497(Pt 2):349–364.
Heginbotham, L., and R. MacKinnon. 1993. Conduction properties of the cloned Shaker K^+ channel. *Biophys. J.* 65:2089–2096.
Imoto, K., C. Busch, B. Sakmann, M. Mishina, T. Konno, J. Nakai, H. Bujo, Y. Mori, K. Fukuda, and S. Numa. 1988. Rings of negatively charged amino acids determine the acetylcholine receptor channel conductance. *Nature.* 335:645–648.
Jiang, Y., and R. MacKinnon. 2000. The barium site in a potassium channel by x-ray crystallography. *J. Gen. Physiol.* 115:269–272.
Kääb, S., H.B. Nuss, N. Chiamvimonvat, B. O'Rourke, P.H. Pak, D.A. Kass, E. Marban, and G.F. Tomaselli. 1996. Ionic mechanism of action potential prolongation in ventricular myocytes from dogs with pacing-induced heart failure. *Circ. Res.* 78:262–273.
Kielland, J. 1937. Individual activity coefficients of ions in aqueous solutions. *J. Am. Chem. Soc.* 59:1675–1678.
Klein, B.K., C.F. Anderson, and M.T. Record. 1981. Condensation model expressions for the colligative properties of cylindrical polyions. *Biopolymers.* 20:2263–2280.
Konno, T., C. Busch, E. Von Kitzing, K. Imoto, F. Wang, J. Nakai, M. Mishina, S. Numa, and B. Sakmann. 1991. Rings of anionic amino acids as structural determinants of ion selectivity in the acetylcholine receptor channel. *Proc. R. Soc. Lond. B. Biol. Sci.* 244:69–79.
Krapivinsky, G., I. Medina, L. Eng, L. Krapivinsky, Y. Yang, and D.E. Clapham. 1998. A novel inward rectifier K^+ channel with unique pore properties. *Neuron.* 20:995–1005.
Kubo, Y., T.J. Baldwin, Y.N. Jan, and L.Y. Jan. 1993. Prmary structure and functional expression of a mouse inward rectifier potassium channel. *Nature.* 362:127–133.
Lopatin, A.N., and C.G. Nichols. 1996. $[K^+]$ dependence of polyamine-induced rectification in inward rectifier potassium channels (IRK1, Kir2.1). *J. Gen. Physiol.* 108:105–113.
Lu, Z., and R. MacKinnon. 1994. A conductance maximum observed in an inward-rectifier potassium channel. *J. Gen. Physiol.* 104:477–486.
MacInnes, D.A. 1961. The Principles of Electrochemistry, New edition. Dover, New York. 478 pp.
MacKinnon, R., and C. Miller. 1989. Functional modification of a Ca^{2+}-activated K^+ channel by trimethyloxonium. *Biochemistry.* 28: 8087–8092.
MacKinnon, R., R. Latorre, and C. Miller. 1989. Role of surface electrostatics in the operation of a high-conductance Ca^{2+}-activated K^+ channel. *Biochemistry.* 28:8092–8099.
Makhina, E.N., A.J. Kelly, A.N. Lopatin, R.W. Mercer, and C.G. Nichols. 1994. Cloning and expression of a novel human brain inward rectifier potassium channel. *J. Biol. Chem.* 269:20468–20474.
Manning, G.S. 1978. The molecular theory of polyelectrolyte solutions with applications to the electrostatic properties of polynucleotides. *Q. Rev. Biophys.* 11:179–246.
Matsuda, H. 1991. Effects of external and internal K^+ ions on magnesium block of inwardly rectifying K^+ channels in guinea-pig heart cells. *J. Physiol.* 435:83–99.
McLaughlin, S. 1977. Electrostatic potentials at membrane-solution interfaces. *Curr. Top. Membr. Transp.* 9:71–144.
McLaughlin, S.G., G. Szabo, G. Eisenman, and S.M. Ciani. 1970. Surface charge and the conductance of phospholipid membranes. *Proc. Natl. Acad. Sci. USA.* 67:1268–1275.
Moczydlowski, E., O. Alvarez, C. Vergara, and R. Latorre. 1985. Effect of phospholipid surface charge on the conductance and gating of a Ca^{2+}-activated K^+ channel in planar lipid bilayers. *J. Membr. Biol.* 83:273–282.
Morais-Cabral, J.H., Y. Zhou, and R. MacKinnon. 2001. Energetic optimization of ion conduction rate by the K^+ selectivity filter. *Nature.* 414:37–42.
Murata, Y., Y. Fujiwara, and Y. Kubo. 2002. Identification of a site involved in the block by extracellular Mg^{2+} and Ba^{2+} as well as permeation of K^+ in the Kir2.1 K^+ channel. *J. Physiol.* 544:665–677.
Nakayama, H., K. Tanizawa, and Y. Kanaoka. 1970. Modification of carboxyl groups in the binding sites of trypsin with the Meerwein reagent. *Biochem. Biophys. Res. Commun.* 40:537–541.
Neyton, J., and C. Miller. 1988. Potassium blocks barium permeation through a calcium-activated potassium channel. *J. Gen. Physiol.* 92:549–567.
Nimigean, C.M., J.S. Chappie, and C. Miller. 2003. Electrostatic tuning of ion conductance in potassium channels. *Biochemistry.* 42:9263–9268.
Park, J.B., H.J. Kim, P.D. Ryu, and E. Moczydlowski. 2003. Effect of phosphatidylserine on unitary conductance and Ba^{2+} block of the BK Ca^{2+}-activated K^+ channel: re-examination of the surface charge hypothesis. *J. Gen. Physiol.* 121:375–397.
Parsons, S.M., L. Jao, F.W. Dahlquist, C.L. Borders Jr., J. Racs, T. Groff, and M.A. Raftery. 1969. The nature of amino acid side chains which are critical for the activity of lysozyme. *Biochemistry.* 8:700–712.
Plaster, N.M., R. Tawil, M. Tristani-Firouzi, S. Canun, S. Bendahhou, A. Tsunoda, M.R. Donaldson, S.T. Iannaccone, E. Brunt, R. Barohn, et al. 2001. Mutations in Kir2.1 cause the developmental and episodic electrical phenotypes of Andersen's syndrome. *Cell.* 105:511–519.
Pogwizd, S.M., K. Schlotthauer, L. Li, W. Yuan, and D.M. Bers. 2001. Arrhythmogenesis and contractile dysfunction in heart failure: roles of sodium-calcium exchange, inward rectifier potassium current, and residual β-adrenergic responsiveness. *Circ. Res.* 88:1159–1167.
Puglisi, J.L., S.M. Pogwizd, W. Yuan, and D.M. Bers. 2000. Increased Na/Ca exchange and reduced IK1 facilitate triggered action potentials in a rabbit model of heart failure. *Biophys. J.* 78:55A.
Qi, X., P. Varma, D. Newman, N. Mamalias, and P. Dorian. 2002. Terikalant and barium decrease the area of vulnerability to ventricular fibrillation induction by T-wave shocks. *J. Cardiovasc. Pharmacol.* 39:242–250.
Reuveny, E., Y.N. Jan, and L.Y. Jan. 1996. Contributions of a negatively charged residue in the hydrophobic domain of the IRK1 inwardly rectifying K^+ channel to K^+-selective permeation. *Biophys. J.* 70:754–761.
Sharp, K., R. Fine, and B. Honig. 1987. Computer simulations of the diffusion of a substrate to an active site of an enzyme. *Science.* 236:1460–1463.
Sigworth, F.J. 1980. The variance of sodium current fluctuations at the node of Ranvier. *J. Physiol.* 307:97–129.
Sigworth, F.J., and B.C. Spalding. 1980. Chemical modification reduces the conductance of sodium channels in nerve. *Nature.* 283: 293–295.
Stampe, P., J. Arreola, P. Perez-Cornejo, and T. Begenisich. 1998. Nonindependent K^+ movement through the pore in IRK1 potassium channels. *J. Gen. Physiol.* 112:475–484.
Weiss, J.N., and S.T. Lamp. 1989. Cardiac ATP-sensitive K^+ channels. Evidence for preferential regulation by glycolysis. *J. Gen. Physiol.* 94:911–935.
Worley, J.F., III, R.J. French, and B.K. Krueger. 1986. Trimethyloxonium modification of single batrachotoxin-activated sodium channels in planar bilayers. Changes in unit conductance and in block by saxitoxin and calcium. *J. Gen. Physiol.* 87:327–349.
Zobel, C., H.C. Cho, T.T. Nguyen, R. Pekhletski, R.J. Diaz, G.J. Wilson, and P.H. Backx. 2003. Molecular dissection of the inward rectifier potassium current (IK1) in rabbit cardiomyocytes: evidence for heteromeric co-assembly of Kir2.1 and Kir2.2. *J. Physiol.* 550:365–372.